Modeling of coating flows on curved surfaces

L.W. SCHWARTZ and D.E. WEIDNER
Departments of Mechanical Engineering and Mathematical Sciences, University of Delaware, Newark DE 19716, U.S.A.

Abstract. The equations describing the temporal evolution of a thin, Newtonian, viscous liquid layer are extended to include the effect of substrate curvature. It is demonstrated that, subject to the standard assumptions required for the validity of lubrication theory, the surface curvature is equivalent to an applied time-independent overpressure distribution. Within the mathematical model, a variety of substrate shapes, possessing both 'inside' and 'outside' corners, are shown to be equivalent. Starting with an initially uniform coating layer, the evolving coating profile is calculated for substrates with piecewise constant curvature. Ultimately, surface tension forces drive the solutions to stable minimum-energy configurations. For small time, the surface profile history, for a substrate with a single curvature discontinuity, is given as the self-similar solution to a linear fourth-order diffusive equation. Using a Fourier transform, the solution to the linear problem is found as a convergent infinite series. This Green's function generates the general solution to the linearized problem for arbitrary substrate shapes. Calculated solutions to the non-linear problem are suggestive of coating defects observed in industrial applications.

1. Introduction

Many industrial or natural processes involve the flow of thin liquid films. The most immediate application is the coating behavior of liquid paints. A freshly applied liquid film normally has an uneven surface. When surface tension can be considered to be uniform, capillary forces tend to reduce surface irregularities to produce a level film. This is the dominant effect leading to relatively uniform, or level, paint films, and for typical coating thicknesses, is much more important than, for example, gravity. A linear theory involving the use of the lubrication assumption, due to Orchard [1], predicts the rate of capillary-induced leveling and has met with considerable practical success.

The beneficial effect of surface tension, leading to more uniform coating layers, is limited largely to solid surfaces or 'substrates' whose curvature variation is small. Indeed, in regions where the substrate is highly-curved, surface tension can result in defects in the final coating: the coating tends to be thin at outside corners, and to be thick or 'puddled' at inside corners. Moreover, characteristic undulations can be found in the final coating near the corners. Typical corner defects, known as 'fat edges' and 'picture-framing' are illustrated schematically in Kornum and Nielsen [2] and are discussed further by Babel [3]. No quantitative measurements of these corner defects appear to have been reported to date, however. While the fundamental process leading to corner defects can be found in the model of a simple Newtonian liquid, industrially useful coatings are typically shear-thinning. Additionally, compositional changes during drying and species diffusion can lead to surface-tension-gradient or Marangoni effects. The resulting additional force on the liquid coating can modify the levelling history and the final coating distribution, as discussed by Overdiep [4] and Schwartz and Eley [5].

The prediction of the thickness variation of coating liquids is important in chemical and nuclear reactors, largely because of the effect on the heat transfer rate on vessel walls.

Coating flow behavior influences the effectiveness of liquid agrochemicals including insecticides and herbicides. Similar issues are relevant to the decontamination of surfaces. Solid layered thin materials, such as photographic film and certain printed media, are often produced via coating flow procedures. Other specialized areas where coating flow is important include lubricants, adhesives, dyes, masonry treatments, surfactants, and glazes. In the electronics industry, photoresists and television tube optical layers are produced using liquid coatings. A number of biomedical areas involve an understanding of coating flow. These include the thin liquid films on the cornea of the eye and on the linings in the lung. In each of these applications, substrates can be expected to be of complex shape and flows resulting from curvature variation may be of importance.

In the following section the fundamental thin-layer or lubrication evolution equation for a Newtonian liquid is reviewed and modified due to substrate curvature effects. While the treatment is largely restricted to the two-dimensional case, the obvious extension to three-dimensional problems is indicated. Since flows are driven only by substrate curvature variations, differently shaped bodies are found to be have similar flow behavior. A simpler problem is discussed in Section 3; here the governing equation is linearized by assuming that the coating is almost uniform. A self-similar solution is found for a substrate with a single jump discontinuity in curvature. This solution can be used as a Green's function for the linear problem for an arbitrary substrate shape. Section 4 presents numerical solutions to the non-linear problem where a partially-implicit finite-difference method is employed for stability and computational efficiency. Asymptotically, the solution tends to a minimum energy configuration with a coating of vanishing thickness on an outside corner. The final section discusses the modifications necessary to extend the analysis to more adequately model typical coatings, including the modeling of compositional changes during drying and resulting Marangoni effects.

2. Lubrication model for surface-tension-driven flows on curved substrates

Figure 1 shows a thin layer of liquid on an impermeable substrate. (s, n) are local orthogonal coordinates with s being arc-length along the substrate and $n = h(s, t)$ is the layer thickness to be determined. For definiteness, impermeable boundaries are assumed at each end of the flow domain. The local radius of curvature is given by $1/\kappa(s)$.

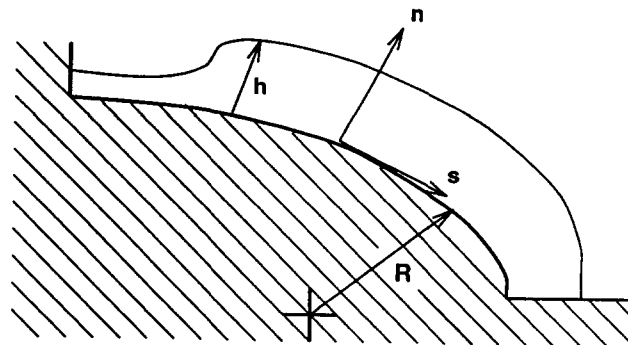The flow of Newtonian or almost Newtonian fluids is governed by the vector Navier–

Fig. 1. Nomenclature and coordinate system.

Stokes equation. Under the assumptions that the fluid layer is thin, the motion is slow, and the free-surface is almost parallel to the substrate, the governing equation may be approximated as

$$-p_s + \mu u_{nn} = 0 \, . \tag{1}$$

Here, subscripts signify partial differentiation, μ is the viscosity and p is the pressure. Equation (1) is the basis of the so-called lubrication theory and its asymptotic validity is well established. (See e.g. Sherman [6].) Because of the thinness of the liquid layer, $p = p(s, t)$ only, and, assuming μ is also independent of n, (1) can be integrated immediately to give a parabolic velocity profile in n. The shear stress at the free surface is equal to the surface tension gradient (see Landau and Lifshitz [7]),

$$\tau_0 = \sigma_s \, ; \tag{2}$$

thus $\partial u / \partial n$ at the free surface is σ_s / μ. For a single-component liquid, in the absence of surface-active material, the surface will be stress free; thus $\tau_0 = 0$. The total flux at any s position is given by

$$Q = \int_0^h u \, \mathrm{d}n$$

and, using (1) and (2) can be written as

$$Q = -p_s h^3 / (3\mu) \, . \tag{3}$$

Since the slope of the free surface is uniformly small, the kinematic boundary condition is $v = h_t$ there, where v is the velocity component in the n direction. Conservation of mass then requires that

$$h_t = -Q_s \, ,$$

yielding, for constant viscosity, the evolution equation

$$h_t = \frac{[h^3 p_s]_s}{3\mu} \, . \tag{4}$$

The pressure within the coating layer can arise from various sources including e.g. body forces due to gravity or centrifugal acceleration. Here we consider only the pressure jump at the free surface due to surface tension σ. Within the lubrication approximation, this is the normal stress boundary condition. From Fig. 2, with subscript '1' signifying quantities at the free surface, we have

$$p = -\sigma\kappa_1 = -\sigma \frac{\mathrm{d}\theta_1}{\mathrm{d}s_1}$$

while, on the substrate,

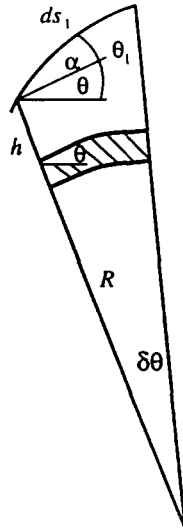$$\kappa = \frac{\mathrm{d}\theta}{\mathrm{d}s} = -\frac{1}{R} \, ,$$

Fig. 2. An element of the substrate and free surface.

where θ is measured from an arbitrary reference direction. (The curvature κ is negative for a convex surface as in Fig. 1.). But, from the figure

$$\theta_1 = \theta + \alpha$$

and, to leading order of infinitesimals,

$$ds_1 = \frac{(R + h)\, d\theta}{\cos \alpha} = \frac{(R + h)\, ds}{R \cos \alpha} .$$

The free-surface curvature may thus be written as

$$\kappa_1 = \frac{d(\theta + \alpha)}{ds(1 + h/R)} \cos \alpha . \tag{5}$$

Assume the free surface inclination, relative to the substrate, is small, i.e.

$$\alpha^2 \ll 1 ; \tag{6}$$

then

$$\cos \alpha \approx 1 - \alpha^2/2 + \cdots \approx 1$$

and

$$\alpha \approx \tan \alpha = dh/ds .$$

If, in addition,

$$h/R \ll 1 , \tag{7}$$

then

$$\kappa_1 = \frac{\mathrm{d}(\theta + h_s)}{\mathrm{d}s} = \kappa + h_{ss} \ . \tag{8}$$

Note that assumption (6) is already required for lubrication theory, while (7) is quite commonly satisfied for coating flows.

The pressure $p = -\sigma\kappa_1$ is seen to be composed of two parts

$$p = -\sigma\kappa - \sigma h_{ss} \tag{9}$$

and, consistent with the lubrication assumption, substrate curvature may be treated as a fixed 'overpressure' distribution. For a substrate corresponding to a three-dimensional body, the equivalent expression is easily seen to be

$$p = -\sigma\kappa - \sigma\nabla^2 h \tag{10}$$

here $\kappa = 1/R_1 + 1/R_2$ is the mean curvature of the substrate and the Laplacian is two-dimensional, in substrate coordinates (s_1, s_2), say.

To explore the consequences of body curvature variation, we formulate a specific initial-boundary value problem. Combining equations (4) and (9), the non-linear evolution equation for the free surface $h(s, t)$ becomes

$$h_t = -(\sigma/3\mu)[h^3(h_{sss} + \kappa_s)]_s \tag{11}$$

with a given forcing function $k_s(s)$. Initially the layer is assumed to be uniform,

$$h(s, 0) = h_0 \ . \tag{12}$$

Symmetry, or no-flow, boundary conditions are imposed at both ends of the flow domain,

$$h_s(0, t) = h_{sss}(0, t) = h_s(L, t) = h_{sss}(L, t) = 0 \ . \tag{13}$$

The initial state is shown schematically in Fig. 3.

Using the non-dimensionalization

$$h = h_0 \hat{h}$$

$$s = L\hat{s}$$
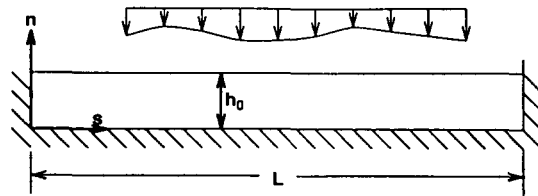
and

$$t = T^* \hat{t}$$

Fig. 3. Initial configuration for curvature-driven coating flow problem. The overpressure distribution corresponding to the curvature is also shown.

where $T^* = 3\mu L^4/(\sigma h_0^3)$, all parameters are removed or absorbed into the forcing function. The evolution equation, replacing (11) becomes

$$\hat{h}_{\hat{t}} = -[\hat{h}^3(\hat{h}_{\hat{s}\hat{s}\hat{s}} + (L/h_0)\hat{k}_{\hat{s}})]_{\hat{s}} \tag{14}$$

while the homogeneous auxiliary conditions remain unchanged. The characteristic time T^* is equivalent to the time scale for leveling of an undulating coating of wavelength L, as predicted by Orchard [1].

We choose, for further investigation, substrates with continuous tangent whose curvature is piecewise constant. There are two reasons for this choice: (i) Typically engineering representations of 'smooth' boundary curves consist of straight lines and circular arcs, with continuous tangent. (ii) While it is clear that if the substrate is taken to be arbitrarily differentiable, the liquid surface, found by the present method, will also be arbitrarily smooth, it needs to be established that the free surface, generated here, will be acceptable when the substrate has curvature discontinuities. Thus, for example, a curvature jump on the liquid surface would imply discontinuous pressure within the liquid layer, which is physically unacceptable. One might, of course, argue that the substrate curvature really is continuous when viewed microscopically. This turns out not to be necessary, however; it will be shown, by the present model, that an initial layer of uniform thickness, possessing discontinuous curvature, will have the discontinuity 'healed' immediately. A substrate with discontinuous curvature is shown in Fig. 4. For this case, or any periodic extension thereof, the evolution equation becomes

$$\hat{h}_{\hat{t}} = -[\hat{h}^3(\hat{h}_{\hat{s}\hat{s}\hat{s}} + M\delta(\hat{s}))]_{\hat{s}} \tag{15}$$

where $\delta(s)$ is the Dirac delta function. With $h(s, 0) = h_0$ and no-flow boundary conditions imposed at $s = -a$ and $s = b$, the dimensionless problem has a two-parameter family of solutions corresponding to prescribed input values of a/b and

$$M = \frac{a^2(\kappa_1 - \kappa_2)}{h_0} \tag{16}$$

Some solutions to this problem, for particular choices of a/b and M, will be given in Section 4.

A wide class of substrate or body shapes are equivalent in terms of coating flow behavior. Corresponding to the same values of a/b and M, and employing reflections in symmetry boundaries, various bodies can be generated. Figure 5 shows several shapes for the particular choice $a/b = 1$ and $a(\kappa_2 - \kappa_1) = \pi/4$. Because $a = b$ for these cases, the similarity class includes coating layers either outside or inside these shapes. The 'unit cell' corresponding to the fundamental curvature distribution, as in Fig. (4b), is shown for each case. All of the bodies shown in Fig. 5 could represent actual curved substrates, which for practical applications, require a painted surface.

For general values of a and b, it can be seen that closed bodies will be generated if

$$a\kappa_1 + b\kappa_2 = 2\pi/n , \quad n = \pm 1, \pm 2 \ldots , . \tag{17}$$

3. A linearized problem

For a uniform coating layer, the flow history, corresponding to equation (15), is driven by the curvature discontinuity on the substrate. For small time, the surface deflection will be
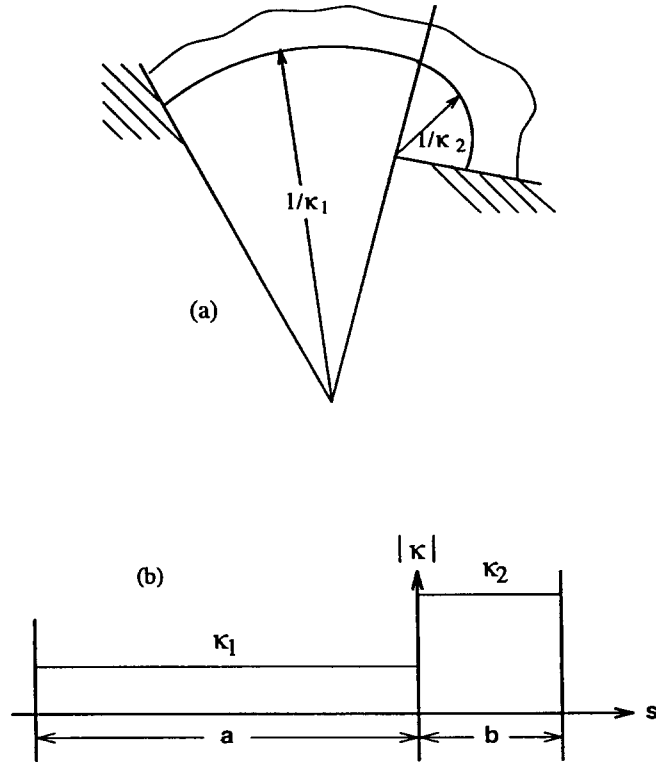
Fig. 4. (a) A substrate composed of two circular arcs with a continuous tangent. (b) The corresponding curvature distribution.
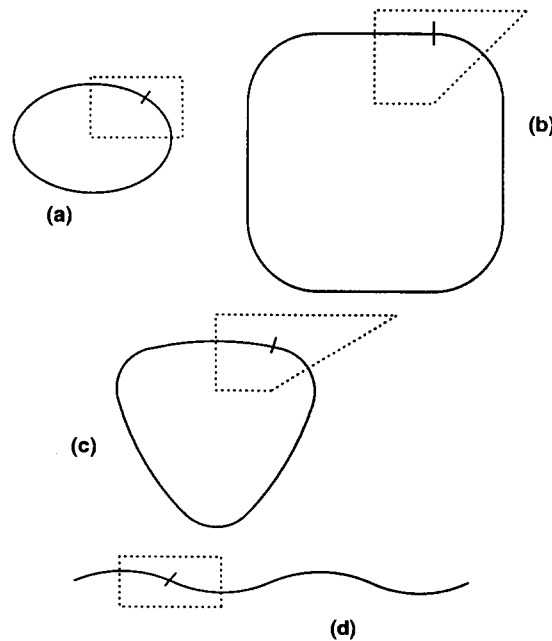

Fig. 5. Similar bodies for coating flow behavior, $a = b$, $a(\kappa_2 - \kappa_1) = \pi/4$. The location of the curvature discontinuity is shown and the dashed line represents the unit cell for each body. Each figure is generated by repeating the unit cell. The coating may be either outside or inside. Parameter values are (a) $a\kappa_1 = \pi/8$, $a\kappa_2 = 3\pi/8$; (b) $a\kappa_1 = 0$, $a\kappa_2 = \pi/4$; (c) $a\kappa_1 = \pi/24$, $a\kappa_2 = 7\pi/24$; (d) $a\kappa_2 = -a\kappa_1 = \pi/8$.

small and will be localized in the neighborhood of this discontinuity. Thus, it is useful to linearize (15) in order to gain information about the analytical character of the solution. For simplicity, we simplify the problem further by imposing the boundary conditions at infinity. Symmetry boundary conditions could, in any event, be recovered by a method of images for the linear problem. We take

$$\hat{h} = 1 + \eta, \qquad \eta \ll 1 \tag{18}$$

and neglect higher-order terms in h. The problem becomes, using dimensionless variables,

$$\eta_t + \eta_{ssss} = -M\delta'(s) \tag{19}$$

subject to the initial condition

$$\eta(s, 0) = 0, \tag{20}$$

and the boundary conditions

$$\eta \to 0 \quad \text{as} \quad s \to \pm\infty. \tag{21}$$

Use of the Fourier transform in s readily yields the solution representation

$$\eta(s, t) = \frac{M}{\pi} \int_0^\infty \frac{1 - e^{-\omega^4 t}}{\omega^3} \sin \omega s \, d\omega \tag{22}$$

which may be seen to be an odd function of s with a curvature discontinuity at $s = 0$,

$$\lim_{s \to 0\pm} \eta_{ss} = \pm \frac{M}{2}. \tag{23}$$

This discontinuity is to be expected since h represents the free surface relative to the substrate. Since the curvature of the substrate is discontinuous at $s = 0$, the discontinuity in η_{ss} makes the curvature continuous for the actual free surface. Inspection of (15) verifies that the non-linear problem must have the same discontinuity.

The function $h(s, t)$ can be expressed as a convergent power series whose coefficients are found explicitly. The integral in (22) is simplified by differentiation with respect to t to yield

$$\eta_t = \frac{M}{\pi} \int_0^\infty \omega \, e^{-\omega^4 t} \sin \omega s \, d\omega. \tag{24}$$

The sine term is then expanded in a power series and the integration with respect to ω is performed term-by-term. The resulting series is integrated with respect to t yielding

$$\eta = \frac{M}{\pi} \sqrt{t} \sum_{n=1}^\infty \frac{(-1)^{n-1} \Gamma\left(\dfrac{2n+1}{4}\right)}{(3 - 2n)(2n - 1)!} \left[\frac{s}{t^{1/4}}\right]^{2n-1} + G(s) \tag{}$$

where Γ is the gamma function and $G(s)$ is an arbitrary function of integration. $G(s)$ is evaluated using (23) and the solution may then be written, in similarity form, as

$$\eta(s, t) = -(M/\pi)t^{1/2} F(\xi) \tag{25}$$

where

$$\xi = s/t^{1/4} ,$$ (26)

and

$$F(\xi) = -\sum_{n=1}^{\infty} \frac{(-1)^{n-1}\Gamma\left(\dfrac{2n+1}{4}\right)}{(3-2n)(2n-1)!} \, \xi^{2n-1} + \frac{\pi}{4} \, \xi^2 \, \mathrm{sign}(\xi) .$$ (27)

A graph of $F(\xi)$ using the series solution is shown in Fig. 6 is a numerical solution to the full non-linear problem. The numerical solution was generated using finite-difference approximations in space and time of equation (19) to determine $\eta(s)$ at given time t. s was then scaled by $t^{1/4}$ and η scaled by $(M/\pi)t^{1/2}$ for comparison with the similarity solution $F(\xi)$. Equation (21) was approximated using symmetry boundary conditions at $s = \pm 10$. As expected the solutions are virtually identical. The numerical solution shown here is for $t = 2.0$.

Also shown in Fig. 6 is a numerical solution to the full non-linear problem. In this case $\hat{h}$ as a function of s was determined from a finite-difference time marching scheme for equation (15). For small times the effect of the non-linearity is minimal since the surface is only slightly deflected from the initial state $\hat{h} = 1$. Thus, for $t = 0.1$, the non-linear solution is very close to the linear one. For $t = 2.0$, on the other hand, non-linear effects are clearly present. For example, the profile is no longer an odd function of ξ. Some details of the numerical procedure are given in the next section.

The solution $\eta(s, t)$ to problem (19)–(21) can be used as a Green's function for the problem with arbitrary given curvature variation $\kappa(s)$. If

$$H(s, t) = \eta(s, t; M = 1) ,$$

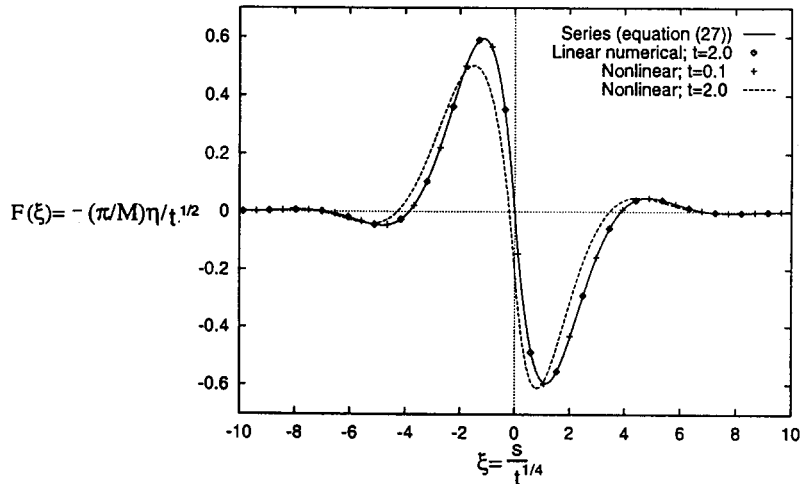and if curvature variation is limited to $a < s < b$, The solution to

Fig. 6. Time evolution of coating thickness in the vicinity of a corner, presented in similarity form. The curvature is discontinuous at $\xi = 0$. There is no visible difference between the analytical solution to the linear problem, given by (27), and a finite-difference numerical solution shown by the symbol $\Diamond$. The numerical scheme is also used for the non-linear problem (15). Non-linear effects are apparent at the larger of the two times shown.

$$y_t + y_{ssss} = -\kappa''(s) \,, \tag{28a}$$

$$y(s, 0) = 0 \,, \tag{28b}$$

$$y \rightarrow 0 \quad \text{as} \quad s \rightarrow \pm\infty \,, \tag{28c}$$

may be expressed as

$$y(s, t) = \int_a^b \kappa'(\zeta) H(s - \zeta, t) \, d\zeta \,. \tag{29}$$

Linear and non-linear equations of higher-order diffusive type are of interest in fields other than fluid mechanics, including metallurgy, flame propagation, and dynamical systems theory (see King [8]; Brand and Deisslen [9]). Consequently this Green's function may be of more general utility.

4. Numerical solutions for coating flows on curved surfaces

A numerical solution to problem (14) can be readily obtained using a finite-difference method. It is desirable, for computational efficiency, to employ a partially-implicit technique, a fully-explicit method being limited to time steps satisfying the inequality

$$\Delta t < O(\Delta s^4) \,. \tag{30}$$

This limitation can be overcome by averaging $h(s, t)$ at the old and new time levels, i.e. using central-differences in time. It suffices to evaluate the nonlinear prefactor h^3 at the old time level, resulting in a pentadiagonal system of linear equations to be solved for each time step. Compared to a simple explicit method, computational requirements can be reduced by perhaps a factor of one thousand without loss of accuracy. The method is described more fully in Moriarty et al [10].

Figure 7 shows the result of a computation on an outside corner for the substrate shown in Fig. (5b). The calculated results, verified to be converged under spatial and temporal refinement, were produced in less than one minute on a desk-top workstation. The solution is equally valid, for either outside or inside coatings, for any other body in the similarity class, as explained in section 2. For convenience, the results are presented in physical units and the values of the input parameters are given in the figure caption. The coating layer thickness variation, at the three times shown, is drawn by projecting $h(s, t)$ normally, from the substrate, at each point on the substrate. The coating thickness has been exaggerated by a factor of 3 for improved visibility; this results in some distortion of the profile, particularly at the last time shown.

The initial coating in Fig. 7 is uniform with a thickness h_0 equal to 0.01 cm (100 μm). Relative to the initial profile, the short time profile (corresponding to $t = 0.03$ seconds) shows the damped oscillations as predicted by the linear problem and shown in Fig. 6. For t equal to 300 seconds, the coating has thinned to a very small value over a portion of the corner arc. The profile is very close to the final steady-state solution, which is approached asymptotically as t tends to infinity. The steady-state solution must be one of minimum energy or minimum surface arc length. The lubrication approximation need not be used here since the final surface is the solution of an elementary isoperimetric variational problem (see e.g. Weinstock
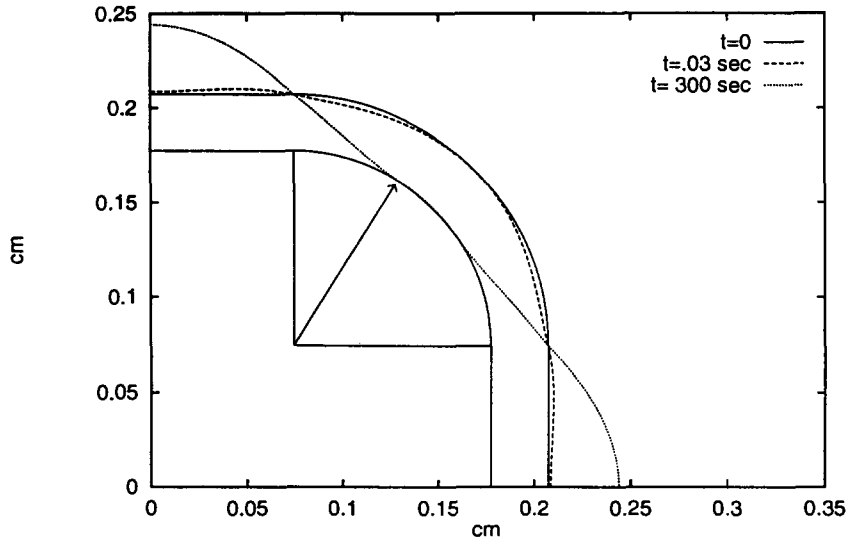
Fig. 7. Coating flow on an outside corner. $\sigma = 30\,\text{dynes/cm}$; $\mu = 1$ poise; $R_c = 0.1\,\text{cm}$; $a = b = 0.0785\,\text{cm}$. Coating thickness scaled by a factor of 3. The ultimate point of tangency, from equation (31), is indicated by the arrow in the figure.

[11]). The final surface must be a circular arc enclosing the initial liquid area. The minimization criterion, applied to the free end-point, requires that the liquid surface must be tangent to the substrate at the point of contact. This condition, that the contact angle must be zero, follows from the fact that, at any finite time, the portion of the arc to be 'de-wetted' still contains some liquid. A similar drainage problem, on a flat substrate, is discussed by Tuck and Schwartz [12]. The point of tangency for the final (exact) profile is located at an angle α, measured from the corner shoulder. α is a solution to the transcendental equation

$$\frac{1}{2}\left(\frac{\alpha}{\sin^2\alpha} - \frac{1}{\tan\alpha}\right) + \frac{R_c}{a}\left(\frac{\alpha}{\sin\alpha} - 1\right) = \frac{h_0}{a}\left(1 + \frac{\pi}{4}\frac{R_c}{a} + \frac{\pi}{8}\frac{h_0}{a}\right). \tag{31}$$

Here R_c is the corner radius. Using the parameters of Fig. 7, α is calculated to be $31.8°$. The location of this point of tangency is shown in the figure, serving as a test of the accuracy of the lubrication calculation.

For comparison, a larger body, but with the same corner radius, is shown in Fig. 8. The damped character of the small time solution is clearly illustrated. At $t = 100$ seconds, the last time is shown, a small, but significant, quantity of fluid remains on the corner. Note that the layer is thinnest near the point of incipient tangency suggesting that the corner coating will thin only very slowly. The ultimate tangency point, calculated for this case to be located at $\alpha = 6.8°$, is also shown in the figure.

5. Concluding remarks

The present paper has given the modifications necessary to adapt free-surface lubrication theory for the calculation of thin-layer flows on curved surfaces. Only a single-component, non-evaporating, Newtonian liquid has been considered here. The thinning of the layer on outside corners and, equivalently, the thickening on inside corners, as found here, is
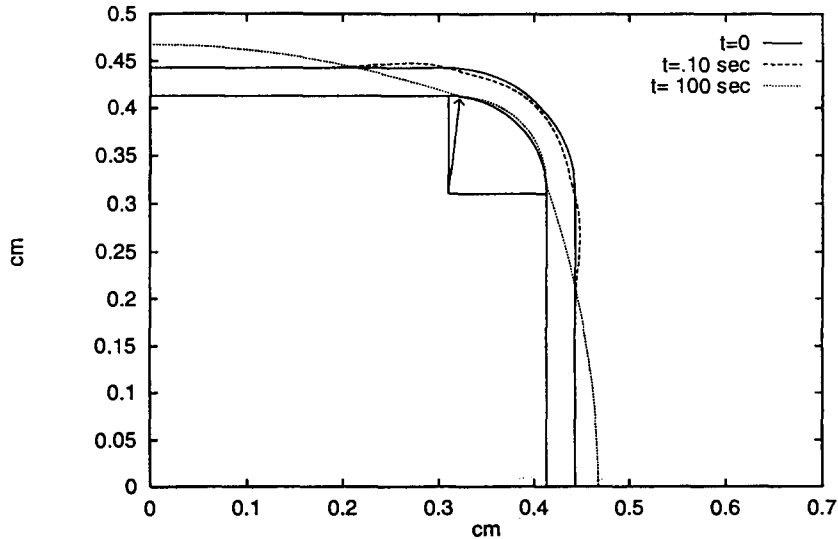
Fig. 8. Coating flow on an outside corner. $\sigma = 30$ dynes/cm; $\mu = 1$ poise; $R_c = 0.1$ cm; $a = 0.3141$ cm; $b = 0.0785$ cm. Coating thickness scaled by a factor of 3. The ultimate point of tangency, from equation (31), is indicated by the arrow in the figure.

suggestive of observed behavior. Most liquids, including all industrially useful coatings, are volatile to some extent; thus the simple theory presented here is incomplete, particularly for large time.

In further work, to be reported upon shortly, we have extended the numerical model to consider a binary mixture with one volatile component. The viscosity of the liquid is no longer constant but can be expected to increase as evaporation proceeds, leading, ultimately, to a dry final film. The necessary modifications include the calculation of the concentration of the non-volatile component as a function of position and time, as well as the variation of viscosity with concentration. Because industrial coatings are typically shear-thinning, the viscosity is also considered to be a function of strain rate. Details of the extended model, and some calculated results for flat substrates, can be found in Schwartz and Eley [5].

Often surface tension is not constant but depends on liquid composition and also on the amount of surface-active material, if present. Resulting surface tension gradients produce a stress distribution on the liquid surface, as given by equation (2), and change the flow history. For systems where compositional changes cause surface tension gradients, the nature of these corner defects, as calculated in this report, can be modified. In particular, our recent work has shown that, if the evaporation time scale is suitably matched to the time scale for flow induced by surface tension gradients, corner defects can be substantially mitigated. While the coating layer thins rapidly at outside corners, as demonstrated here, with suitably chosen parameters the liquid can be pulled back to the corner before it dries, producing a nearly-uniform final coating.

Acknowledgements

References

1. S.E. Orchard, Surface levelling in viscous liquids and gels. *Appl. Sci. Res. A* 11 (1962) 451–464.
2. L.O. Kornum and H.K. Raashou Nielsen, Surface defects in drying paint films. *Prog. in Organic Coatings* 8 (1980) 275–324.
3. E. Babel, *Plaste Kautsch.* 21 (1974) 695–698.
4. W.S. Overdiep, The leveling of paints. *Prog. in Organic Coatings* 14 (1986) 159–175.
5. L.W. Schwartz and R.R. Eley, Numerical simulation of post-application coating flows, including flows arising from surface tension gradients. Submitted to *Prog. in Organic Coatings.*
6. F.S. Sherman, *Viscous Flow.* McGraw-Hill, New York (1990).
7. L. Landau and E. Lifshitz, *Fluid Mechanics.* Pergamon, Oxford (1959).
8. J.R. King, Integral results for nonlinear diffusion equations. *J. Eng. Math.* 25 (1991) 191–205.
9. H.R. Brand and R.J. Deissler, Noise-sustained structures, confined states and convective instability, In: F. Moss, L.A. Lugiato and W. Schleich (eds), *Noise and Chaos in Non-linear Dynamical Systems.* Cambridge University Press (1990) 125–141.
10. J.A. Moriarty, L.W. Schwartz and E.O. Tuck, Unsteady spreading of thin liquid films with small surface tension. *Physics of Fluids A* 3 (1991) 733–742.
11. R. Weinstock, *Calculus of Variations.* McGraw-Hill, New York (1974).
12. E.O. Tuck and L.W. Schwartz, Thin static drops with a free attachment boundary. *J. Fluid Mech.* 223 (1991) 313–324.